Article

A2B-Miktoarm Glycopolymer Fibers and Their Interactions with Tenocytes

Renjie Liu, Dharmesh Patel, Hazel R.C. Screen, and C. Remzi Becer

Bioconjugate Chem., **Just Accepted Manuscript** • DOI: 10.1021/acs.bioconjchem.7b00279 • Publication Date (Web): 21 Jun 2017

A_2B-Miktoarm Glycopolymer Fibers and Their Interactions with Tenocytes

Renjie Liu[†], *Dharmesh Patel*[‡], *Hazel R.C. Screen*[‡*], *C. Remzi Becer*[†*]

[†]Polymer Chemistry Laboratory, School of Engineering and Materials Science, Queen Mary, University of London, E1 4NS London, United Kingdom

[‡]Institute of Bioengineering, School of Engineering and Materials Science, Queen Mary, University of London, E1 4NS London, United Kingdom

Corresponding authors: r.becer@qmul.ac.uk and h.r.c.screen@qmul.ac.uk

ABSTRACT: Electrospun biodegradable membranes have attracted great attention for a range of tissue engineering applications. Among them, poly (ε-caprolactone) (PCL) is one of the most widely used polymers, owing to its well-controlled biocompatibility and biodegradability. However, PCL also has a number of limitations, such as its hydrophobic nature and the lack of functional groups on its side chain, limiting its ability to interact with cells. Herein, we have designed and prepared a series of well-defined A_2B-miktoarm copolymers with PCL and glycopolymer segments to address these limitations. Moreover, copolymers were electrospun to make membranes, which were studied *in vitro* to investigate cell affinity, toxicity, activity and adhesion with these materials. The results indicate that incorporating glucose moieties into miktoarm polymers have significantly reduced the toxicity of the PCL while increasing the cellular interaction with the membrane material.

Keywords: PCL**;** glycopolymers; tenocyte; cell attachment, biocompatibility

Introduction

Tissue regeneration is a major focus in the field of tissue engineering. Current approaches tend to adopt membranes or scaffolds to direct tissue repair, generally requiring cell-material interactions[1, 2]. Tissues like tendon[3], skin[4] and bone[5], have a 3D hierarchical structure comprised of fibrils or fibres with a size range from nanometres to millimetres. Thus, nano-scale 3D scaffolds have been extensively used to mimic the matrix of human tissue for biological applications[6, 7]. 3D scaffolds have been used in bone[8], tendon[9], skin[10], cartilage[11] and blood vessel related applications[12], and 3D scaffolds fabricated via electrospinning[13], phase separation[14] or self-assembly[15]. Among those methods, electrospinning is the most widely used approach due to its simplicity and the formation of well-organised 3D porous structures[16].

With the advancement of polymer chemistry, well-defined polymer membranes have been increasingly used in biological applications[17-19]. Among biodegradable polymers, polyesters have been the most widely investigated and used. For example, poly(lactic acid) (PLA)[20], poly(glycolic acid) (PGA)[21], polycaprolactone (PCL)[22] and their copolymers[23, 24] have all been used in clinical applications such as surgical sutures[25], fixation devices[26] and tissue regeneration scaffolds[27]. The popularity of these polymers stems not only from their biocompatibility and biodegradability, but also because they are some of the few synthetic polymers that are currently approved by the U.S. Food and Drug Administration (FDA) for human clinical applications. Of the polyester family, PCL is one of the most widely used biodegradable polymers, due to its long degradation time and well retained structure *in vivo*[28]. However, the use of PCL is limited by the high hydrophobicity of its polymer backbone, which lowers its ability to interact with cells[29]. To address this, many natural compounds, such as chitosan[30], collagen[31, 32]and carbohydrates[33] have been used to modify the surface of PCL to promote cell attachment. However, the fast release of the physically blended

bioactive molecules from PCL *in vivo* has limited the long-term applications[34]. Therefore, a number of recent studies have focused on incorporating carbohydrates into polymers by modifying the polymer backbone with functional groups. The resulting carbohydrate rich materials, often referred to as glycopolymers, interact more readily with cells[35],offering potential applications in drug delivery nanoparticles[36], capsules[37], sponges[38] and fibres[39].

It is known that the architecture of a polymer has a significant effect in biological applications. For instance, complex miktoarm star shaped polymers show significantly higher uptake of cells in drug delivery[40, 41], or gene delivery[42, 43] vehicles, and due to the improvement of the nano particle stability[44], star polymers can even be used for fluorescent tracking systems [45, 46]. At the same time, glycopolymers have gained increasing interest due to their bioactive properties[47] showing better interactions with cells when formed as nanoparticles [48]as well as specific lectin recognition[49]. However, the interactions of miktoarm star shaped glycopolymers with cells have not been well investigated yet.

Tendons connect and transfer the strain from muscle to bone, thus allowing muscles to withstand higher stress. However, tendon injuries are one of the biggest challenges across the world, which occur mostly because of high tendon loads, aging of tendon as well as laceration injuries for tendon in hand[50, 51]. Nonetheless, reconstruction of tendon after injury is still challenging due to the poor interaction between the scaffolds and tenocytes, which synthesize collagen and secret growth factors, restricts the healing of tendon. Thus a high cell affinity tissue engineering platform is demanding.

In this study, a naturally abundant carbohydrate, glucose, was incorporated into PCL-based copolymers by a combination of ring opening polymerization (ROP), atom transfer radical polymerization (ATRP) and thio-ene chemistry, to fabricate a 3-arm glycopolymer.

The PCL-*block*-glycopolymers were then electrospun to fabricate membranes, for which toxicity, cell attachment and cell activity were investigated, using bovine tenocytes as a cell source.

Results and discussion

Synthesis of PCL and PCL block copolymers.

Star shape polymers can be achieved via arm first[52] and core first[53] strategy. By using a bifunctional initiator, different synthesis techniques can be used in one pot or in sequence to achieve block copolymers. $Sn(Oct)_2$ is one of the most widely used catalyst for the synthesis of high molecule biodegradable polyesters. Para fluorine substitution reaction is one of the most efficient reaction type that can be used to synthesize glycopolymers[54, 55]. Thus PCL homo polymer was synthesized using an initiator with two hydroxyl groups. Then PCL was used as a macro initiator to extend the polymer chain of styrene or PFS. Lastly, 1-Thio-*β*-*D*-glucose was substituted onto PCL-*mikto*-PPFS block copolymer backbone.

A schematic depicting the stages of the reactions is provided in Figure 1. The chemical structure of these polymers were investigated at each stage of this process, and the molecular weight, *Đ* and conversion of the different polymers shown in Table 1, while the GPC trace and NMR of each polymer is shown in Figure 2 and Figure S1.

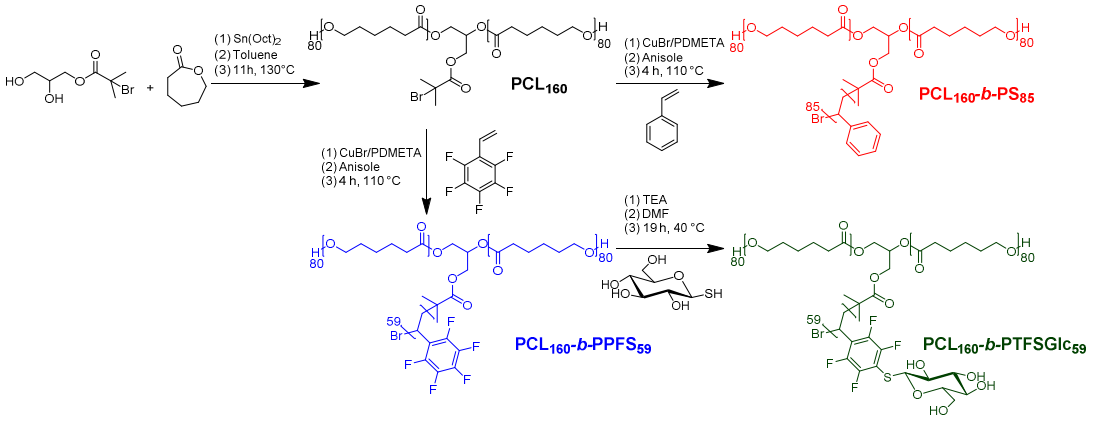

Figure 1. Schematic representation of the synthesis of PCL, block copolymers PCL-*mikto*-PS, PCL-*mikto*-PPFS and PCL-*mikto*-PTFSGlc by ROP of ε-CL and Atom Transfer Radical Polymerization (ATRP) of styrene or PPFS and click reaction with thio-glucose.

GPC analysis and NMR spectroscopy indicate the success of the reactions (**Error! Reference source not found.**). In the GPC traces, a clear shift towards the high molecular weight region was observed (Figure 2A). Meanwhile, ^{1}H NMR spectroscopy showed the appearance of *–CH-CH$_2$-* group in the range of 1.2-3.0 ppm after ATRP reactions, as well as sugar groups in the range of 4.1-6.0 ppm after the sugar moieties were click on to the polymer (Figure 2b). ^{19}F NMR spectroscopy proved the total consumption of all para fluorine after the click reaction. In summary, data confirmed the successful synthesis of PCL, PCL-*mikto*-PS, PCL-*mikto*-PPFS and PCL-*mikto*-PTFSGlc block copolymers (Figure 2, Figure S1).

Table 1. Analysis of PCL, PCL-mikto-PS, PCL-mikto-PPFS and PCL-mikto-PTFSGlc.

Composition[a]	Conversion [%]		$M_{n,theo}$ [g mol^{-1}]	$M_{n,GPC}$[d] [g mol^{-1}]	$Đ$[d]
PCL_{160}	CL	100[b]	11600	18190	1.46
PCL_{160}-*mikto*-PS_{85}	Styrene	70[b]	22420	27350	1.29
PCL_{160}-*mikto*-$PPFS_{59}$	PFS	65[b]	28280	29550	1.51
PCL_{160}-*mikto*-$PTFSGlc_{59}$	Thio-glucose	100[c]	51410	56800	1.45

[a] Calculated by GPC results; [b] Conversion (ρ) measured by ^{1}H NMR; [c] Conversion (ρ) measured by ^{19}F NMR; [d] DMF eluent, PS standards.

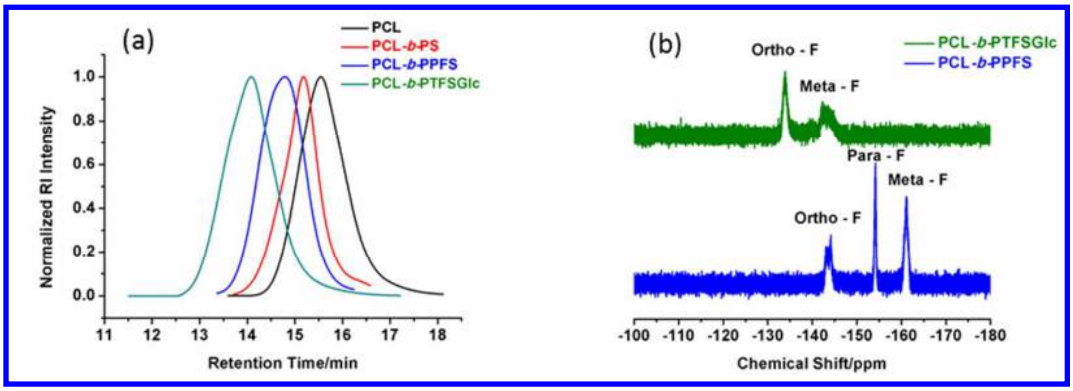

Figure 2. (a) GPC trace of PCL, PCL-*mikto*-PS, PCL-*mikto*-PPFS and PCL-*mikto*-PTFSGlc (*left)*; (b) ^{19}F NMR of PCL-*mikto*-PPFS and PCL-*mikto*-PTFSGlc (*right*).

Characterization of polymer membranes. These polymer solutions were electron spun into four different groups of membranes (Table 1). The surface morphologies of the four different electrospun membranes are shown in Figure 3. The fibres formed a randomly interconnected structure, and appeared to possess a smooth surface at the macro-scale in all membranes. The overall fibre diameter ranged from 0.2-0.6 um, with the variability likely attributed to the solubility of each polymer type in the co-solvent. However, no significant differences in fibre diameters between materials were seen, with average values of 0.34 ± 0.20 μm, 0.33 ± 0.17 μm, 0.32 ± 0.10 μm and 0.34 ± 0.14 μm for the P1-P4 materials, respectively. To clarify the effects of chemical composition on the surface properties of electrospun fibres, the water contact angle with each membrane was measured. Mean water contact angles were 117.42° ± 0.78° for P1, 124.36° ± 0.22° for P2, 123.32° ± 0.36° for P3 and 0° for P4 respectively (Figure 3). Overall, data demonstrated that mixing block copolymers with homo PCL did not significantly influence the average diameter of fibres in electrospun membranes (Figure S2A), but did change the hydrophilicity of the surface significantly (Figure 3, Figure S2B). The incorporation of a hydrophobic block creates a surface, which behaves more hydrophobic and *vice versa*.

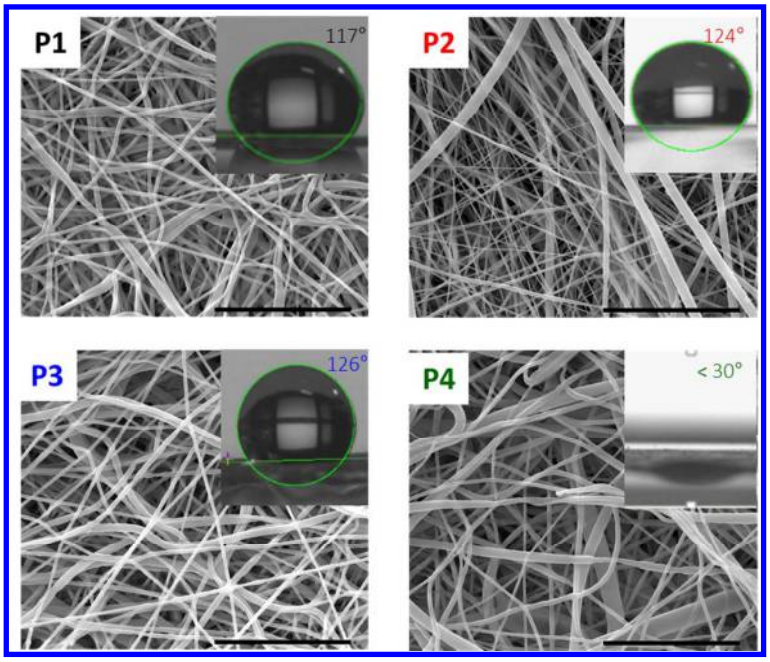

Figure 3. A typical SEM image of each polymer membrane, with inset showing a matched typical water contact angle result. Scale bar represent 10 μm in all pictures.

Results of cell viability and affinity on membranes Aiming at designing a platform which can interact promptly with tendon, which can improve the healing of injury tendon, tenocytes were used as cell line to carry all the *in vitro* tests. The toxicity of the different membranes towards tenocytes was characterised using calcein AM and ethidium homodimer (Figure 4), investigating both cell viability (Figure 5) and cell coverage on the materials (Figure 6). Cell viability was maintained above 60% in all test groups for up to 48 hrs of incubation (Figure 5), No significant differences were evident between any of the test groups, nor between test groups and the positive control, of cells cultured on tissue culture plates.

However, it was notable that cell coverage was significantly improved on P4 membranes relative to P1-P3 membranes (Figure 4 and Figure 6), with coverage on P1-P3 membranes below that seen in negative controls. Taken together, these data suggest that incorporating sugar molecules into the polymer, even at low percentages, can enhance its

interaction with cells. Sugar moieties have been proved to interact promptly with C type lectins[47]. The attraction of these lectins will lead to enhancement of cell attachment on the functional surfaces, which probably accounts for the increase of cell coverage on P4 group.

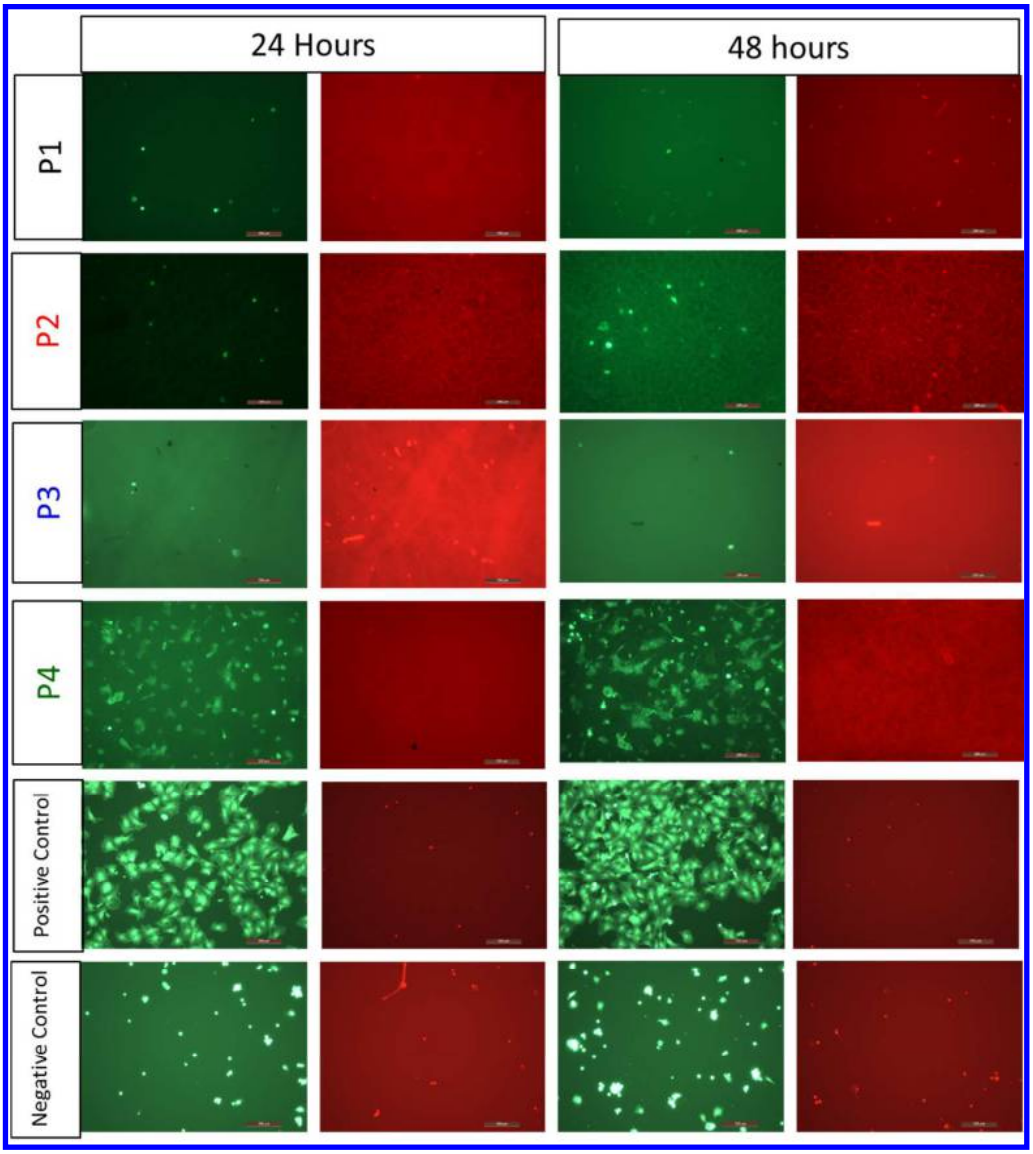

Figure 4. Live/dead assay of tenocytes on different polymer membranes after 24 hours (*left columns*) and 48 hours (*right columns*). Viable cells are shown in green and dead cells in red.

In vitro cell adhesion and morphology. Tenocyte adhesion to each membrane type was assessed by characterising cell morphology on the materials, using phalloidin and DAPI to stain the cytoskeleton green and nucleus blue respectively (Figure 7). Images demonstrate

that tenocytes on the P4 membranes were better adhered, as greater cytoskeleton tension was observed relative to the rounder cells on P1 – P3 membranes. These data further support the hypothesis that the grafted sugar molecules provide the membrane with a functional group which facilitates cell attachment and migration.

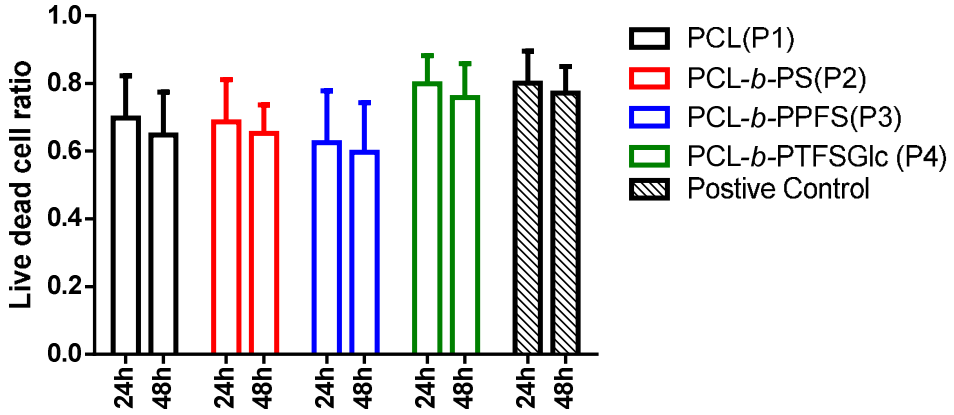

Figure 5. Comparison of cell viability between different membranes and the tissue plastic controls at different time points. Values represent the mean ± SD of all samples (n = 3). Statistical significance was calculated using a one way ANOVA followed by Tukey comparison of means method.

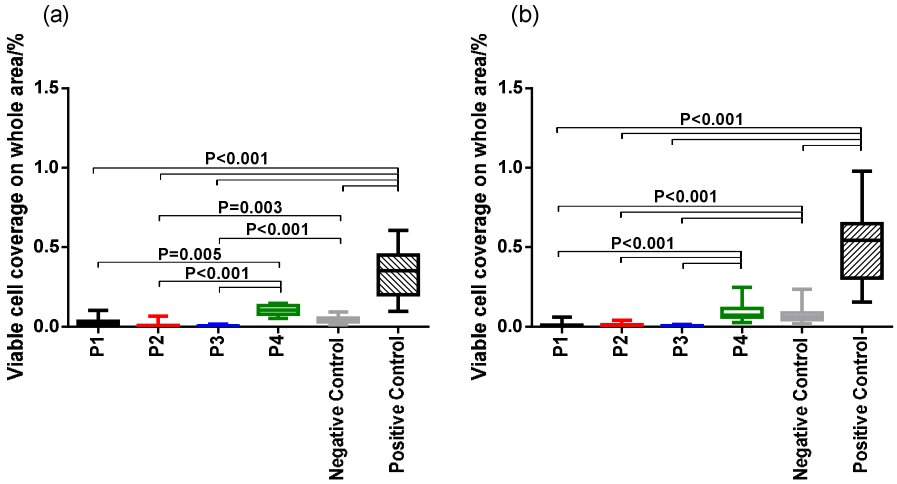

Figure 6. Comparison of viable cell coverage between different membranes and tissue culture plastic controls at the (a) 24 h and (b) 48 h time points. Values represent the mean ± SD (n = 3). Statistical significance was calculated using the Kruskal-Wallis tests followed by Dunn's tests method.

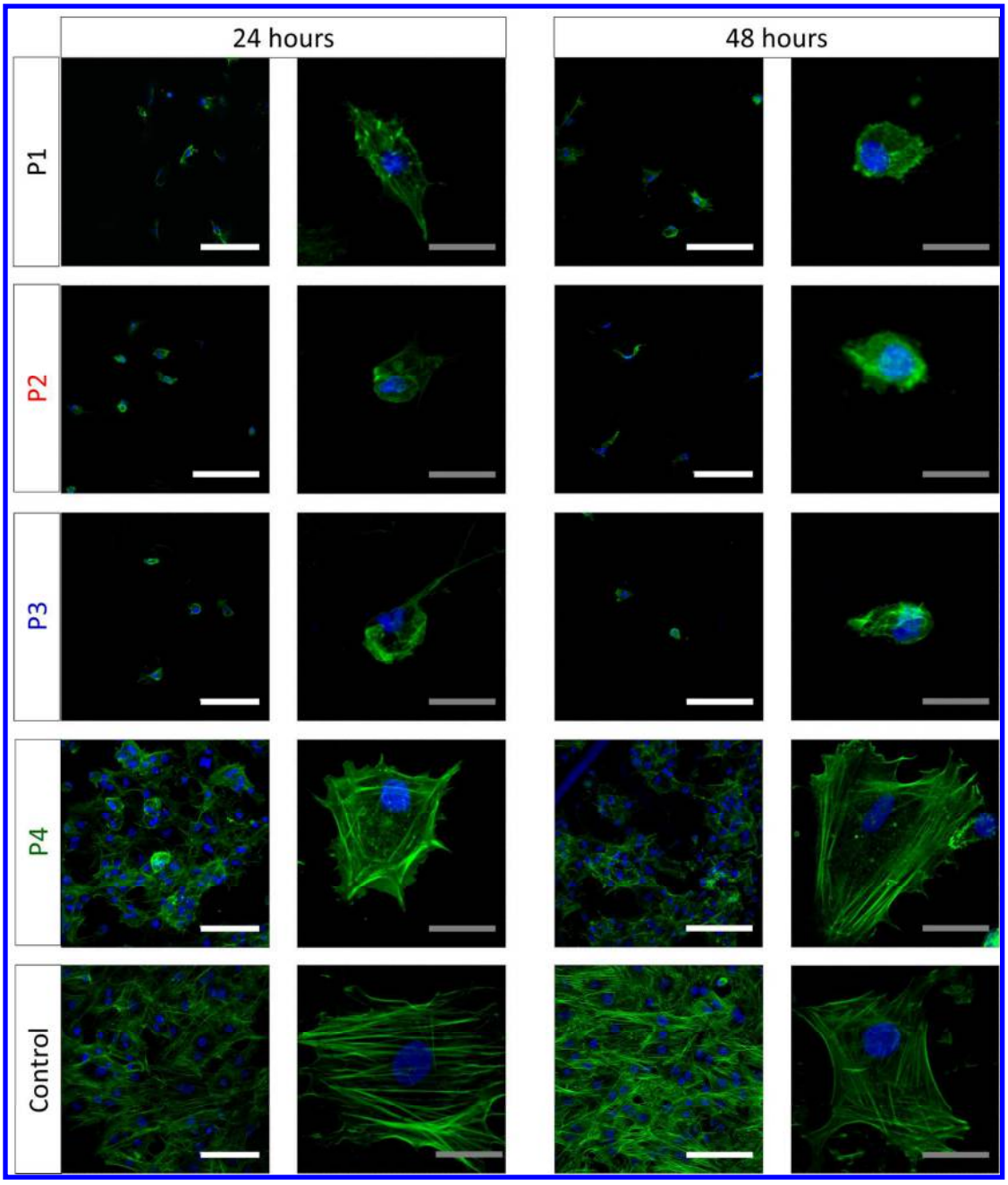

Figure 7. Typical images of tenocytes seeded onto each of the polymer membranes (P1 to P4) and on tissue culture plastic (control). Green staining represents the cytoskeleton while blue represents the nucleus of cells. Images show cells after 24 hours (*left columns*), and 48 hours (*right columns*). Two different magnifications are shown for each condition: the white scale bar represent 100 µm; the grey scale bar represent 25 µm.

Results of alamar blue assay. The influence of different membranes on cell activity was characterised using an alamar blue assay with cell activity calculated relative to that seen in control cells seeded on tissue culture plastic at equivalent time points (control cell activity shown in Figure S3). A trend towards reduced relative cell activity was observed on all the polymer membranes relative to the positive controls for the first 48 hours, after which activity on most membranes tended to increase to either match or surpass that on tissue culture plastic (Figure 8). The activity on PCL was notably lower than in all other materials, and consistently lower than seen in the cell culture plastic controls. It has been shown that incorporation of proteins or growth factors can increase cell activity on the surface[56]. P4 membranes contains sugar moieties, which interact promptly with C-type lectins and then interact actively with cells, thus leads to an increase in cell activity. At the meantime, cells tends to behave more active when can not attach to a surface and try to proliferate off, thus there are also improved cell activity trend in P2-P3 groups.

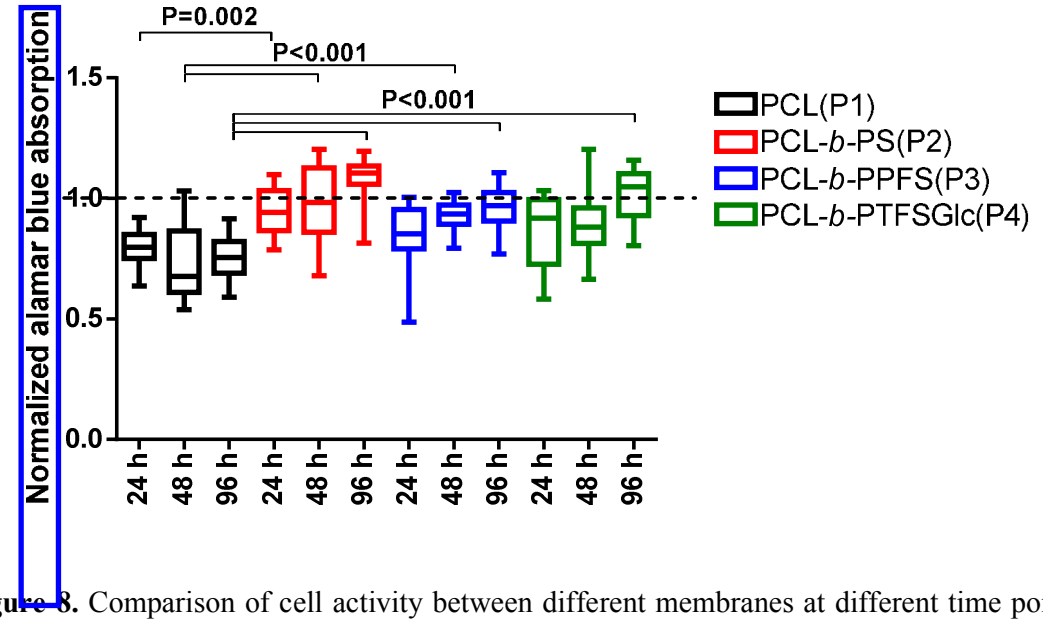

Figure 8. Comparison of cell activity between different membranes at different time points. Values represent the mean ± SD normalized to the activity of control cells (can be seen as dashed line) at the same time (Set as 1.0) (n = 3). The alamar blue results for cell activity of

the control group are shown in Figure S3. Statistical significance was calculated using the Kruskal-Wallis tests followed by Dunn's tests.

Conclusion and outlook

As one of the most widely used materials for tissue engineering, PCL has received considerable attention. However, the interaction between PCL scaffolds and cells has always been poor, due to the hydrophobic nature of the PCL backbone. Studies have attempted to modify PCL to overcome this limitation, mostly focusing on mixing natural or synthetic substances with PCL. However, such blends have a limited use, as the added materials leech out of the PCL. Chemically modification of PCL to covalently bond the functional groups would provide more stable materials. However, to date, chemical modifications of PCL have mostly been limited to Cu-mediated or aminolysis click reactions, which have limited practical uses in biological applications.

The current study aimed to address this, by chemically modifying PCL with glucose moieties, to provide functional sugar groups for cell attachment, through a combination of ROP, ATRP and subsequent thio-ene substitution reactions. 3D membranes of the modified PCL materials were successfully electrospun to make membranes with a tissue mimetic structure which could potentially be used in tissue engineering. The morphology and properties of the membranes were characterised by SEM and an assessment of water contact angle, showing that hydrophilicity of a membrane could be dramatically improved with the addition of sugar groups, without altering the fibre diameters. *In vitro* membrane biocompatibility tests with tenocytes showed that cell attachment capabilities of membranes were significantly improved by incorporating sugar molecules into PCL.

The sugar modified PCL characterised in this study has many potential applications in the tissue engineering field, however, the underlying mechanisms through which cells interact

with sugar molecules, and the influence of sugar content on cell metabolism needs further analysis.

Materials and methods

Materials. Tin(II) 2-ethylhexanoate($Sn(Oct)_2$, 92.5%-100%), DL-1,2-isopropylideneglycerol (98%), α-bromoisobutyryl bromide (98%), trimethylamine (TEA) (BioUltra, ≥99.5%), 1-Thio-*β*-*D*-glucose sodium salt, aluminium oxide (Al_2O_3), toluene anhydrous, ethidium homodimer were purchased from Sigma Aldrich and used as received. *N,N,N',N'',N''*-Pentamethyldiethylenetriamine (PMDETA) was purchased from Acros Organics. DMEM, Dulbecco's phosphate-buffered saline, Alamar Blue® cell viability reagent, Alexa Fluor® 488 Phalloidin, 4',6-Diamidino-2-Phenylindole, Dihydrochloride (DAPI) were purchased from Thermo Fisher and used as received. Calcein AM was purchased from Biotium and used as received. ε-caprolactone (ε-CL) (97%) was purchased from Sigma Aldrich and distilled against calcium hydride before use. Styrene (99.5%, stab. with 4-*tert*-butylcatechol) was purchased from Alfa Aesar and passed over a basic aluminium oxide column to remove inhibitors prior to use. 2,3,4,5,6-pentafluorostyrene (PFS) was purchased from Sigma Aldrich and passed over a basic aluminium oxide column to remove inhibitors prior to use. Cu(I)Br was stirred in acetic acid for 4 h, then filtered and washed with ethanol and dried *in vacuo* prior to use.

High molecular weight homopolymer of PCL (Capa^{TM} 6500D) was kindly provided by Perstorp Winning Formulas Corporation. All other reagents and solvents were purchased from Sigma Aldrich or Fisher Scientific at the highest purity available and used without further purification unless stated otherwise.

Measurements. ^{1}H and ^{19}F Nuclear Magnetic Resonance (NMR) spectra were recorded on a Bruker AVIII 400 using deuterated chloroform ($CDCl_3$) or deuterated dimethyl sulfoxide (DMSO-d_6). Gel Permeation Chromatography (GPC) measurements were carried on an

Agilent 1260 infinity system operating in dimethylformamide (DMF) with 5 mM Ammonium tetrafluoroborate at 40 °C and equipped with refractive index detectors and variable wavelength detectors, 2 PLgel 5 μm mixed-C columns (300 × 7.5mm), a PLgel 5 mm guard column (50 × 7.5mm) and an auto sampler. The instrument was calibrated with linear narrow poly styrene standards in range of 550 to 46 890 g/mol. Some samples were passed through the neutral aluminium oxide and a 0.2 μm Nylon filter before analysis.

Polymer synthesis

Ring opening polymerization of ε-caprolactone. PCL homo polymers were prepared by ring-opening polymerization (ROP) of ε-CL initiated by 2,3-dihydroxpropyl 2-bromo-2-methylpropionate using $Sn(Oct)_2$ as the catalyst in anhydrous toluene following the procedure reported elsewhere[57]. The reaction mixture was added into a dried glass Schlenk tube, previously vacuumed and Argon purged 3 times, and then sealed to maintain an inert atmosphere. The reaction was carried out at 130 ºC for 13 h. The polymer was dissolved in 10 mL of Tetrahydrofuran (THF) and precipitated twice in cold methanol, filtered and the final polymer was dried *in vacuo* at 40 °C overnight. The final PCL homo polymer was obtained as a white powder.

Ring opening polymerization of caprolactone and atom transfer radical polymerization of Styrene or PFS. PCL-mikto-PS and PCL-mikto-PPFS block copolymers were synthesized by ROP of ε-CL and then ATRP of styrene or PFS, respectively. The typical procedure for the synthesis of PS or PPFS starts with degassing the ligand (PMDETA), and 50% of the total amount of anisole for 10 minutes. After degassing, the solution was transferred with a degassed syringe to a Schlenk tube, containing Cu(I)Br in an inert atmosphere. Cu and the ligand mixture in anisole were degassed for further 15 minutes. At the same time, styrene or PFS was purged by nitrogen for 15 minutes and then transferred with a degassed syringe to the catalyst complex mixture. Finally, the degassed macro initiator and solvent mixture were

transferred with a purged syringe to a Schlenk tube, and the mixture purged for another 15 minutes before the reaction started.

The reaction was started by placing the Schlenk tube into an oil bath. The reaction was stopped by bubbling the solution for 3 minutes with air followed by further dilution of the reaction mixture with THF. The final block copolymer was purified by passing the dilute solution through the basic Al_2O_3 column, to remove the Cu^0 formed during reactions. The polymer was then precipitated in cold methanol ($pH \approx 3$), filtered, and the final block copolymer was dried *in vacuo* at 40 °C overnight, from which a white powder was obtained.

Click reaction of the block copolymer and 1-Thio-β-D-glucose. The general method for performing the click reaction has been reported elsewhere and was adopted here, with a modification to the reaction time only[55]. In brief, the click reaction mixed PCL-*mikto*-PPFS copolymer (1.00 g, 2.37 mmol) with the protected sugar (510 mg, 2.37 mmol) dissolved in 8 mL of dry DMF. TEA (1.00 mL, 7.02 mmol) was added to the reagent solution as a catalyst. The reaction mixture was stirred for 20 h at 40 °C, concentrated to 2.5 mL, precipitated into cold methanol twice, and filtered. The final block copolymer PCL-*mikto*-PTFSGlc was dried *in vacuo* at 40 °C overnight and obtained as a white powder.

Preparation of polymer electrospinning solution. PCL-*mikto*-PS, PCL-*mikto*-PPFS, PCL-*mikto*-PTFSGlc were blend with PCL (Capa™ 6500D) in 1:4 ratio, to prepare four different solutions (P1 to P4) as outlined in Table 1, for electrospinning into membranes.

Table 2. Composition of solutions for electrospun membranes.

Code	Solution composition	Solvent ratio
P1	PCL (Capa™ 6500D)	$CHCl_3$: DMF (*w/w* = 1:3)
P2	PCL-*mikto*-PS: PCL (Capa™ 6500D)= (*w/w* = 1:4)	$CHCl_3$: DMF (*w/w* = 1:3)
P3	PCL-*mikto*-PPFS: PCL (Capa™ 6500D)= (*w/w* = 1:4)	$CHCl_3$: DMF (*w/w* = 1:3)
P4	PCL-*mikto*-PTFSGlc: PCL (Capa™ 6500D)= (*w/w* = 1:4)	EF: DMF (*w/w* = 1:3)

All the solutions were stirred for at least 6 h prior to electrospinning. EF: Ethyl formate

Electrospinning. Each polymer blend solution was electrospun in turn. The solution was placed in a plastic syringe (5 ml, Injekt®, Braun, Germany) and connected to a metal syringe needle (0.8 mm diameter), and then Polytetrafluoroethylene (PTFE) syringe tube (20 gauge) on the pump (Genie, Kent Scientific Corporation, USA). Electrospinning was performed at a high voltage of 25 kV, supplied directly from a high DC voltage power supply (0-30kV, Glassman High Voltage, Inc., Whitehouse Station, NJ) and the resulting membranes were collected through a steel plate 10-15 cm away from the tip of the syringe needle on a static aluminium foil. Membranes were dried in a vacuum oven at 40 °C overnight before further use. In total, three membranes, approximately 300mm x200 mm were made for each sample solution (P1 to P4) for further analysis.

Characterization of polymer membranes. The morphology of one sample of each electrospun membrane was observed by scanning electron microscopy (SEM) (Inspect F, FEI, Netherlands). Three discs (5mm diameter) were punched from the membrane, and prepared for SEM. For each disc, at least three images were taken at different random locations across the sample, and fibre diameter was characterised across these, by measuring the diameter of at least 100 fibres in total using Image J (ImageJ software, NIH Image, MD, U.S.A.). A

single value (mean ± standard deviation (SD)) is presented for fibre diameter in each membrane.

Surface wettability was also determined from a small region of all three of each type of electrospun membrane (P1-P4). Three discs (5 mm diameter) were cut from each three of the electrospun membranes. Surface wettability of each material was evaluated by the water contact angle (WCA) method at room temperature. Water contact angle of a sessile drop was measured with a Kruss DSA100 (Hamburg, Germany) using the inbuilt with DSA 1.9 software. For each disc, at least five measurements were taken at different locations across the surface area, giving a total of 15 measures of water contact angle per membrane with the results presented as mean ± SD.

Polymer membrane and cell preparation for in vitro tests. 45 discs (15mm diameter) were cut from the remaining two membranes using a punch for the different in vitro cell biocompatibility tests. All discs were sterilized by immersion in 70% ethanol overnight, and irradiated under UV light, after which they were washed repeatedly with sterile PBS to remove residual ethanol prior to cell seeding.

Tenocytes isolated from bovine extensor tendons via tissue digestion (1 U/mL dispase and 2 mg/mL collagenase type II for 24 h at 37 °C) were adopted as a cell source[58]. Tenocytes were cultured in Dulbecco's Modified Eagle Medium (DMEM) (low glucose, pyruvate) supplemented with 10% (v/v) bovine serum, 100 U/mL penicillin, 1 % (v/v) nonessential amino acids, 2% (v/v) N-2-hydroxyethylpiperazine-*N*-2-ethane sulfonic acid (HEPES), 0.37% (w/v) sodium bicarbonate and 1% (v/v) L-glutamine, at 37 °C, 5% CO_2 in a humidified incubator. The culture medium was changed every 2 days and cells maintained until use at passage 3, when they were harvested using trypsin-EDTA (0.25% trypsin) [58].

Cell viability and affinity on membranes. Six sterilized discs of each membrane material (P1-P4) were placed, one disc per well, into the wells of a non cell culture-treated 24-well plate, and cell solution pipetted directly onto the discs, in order to seed them at a density of 1×10^4 cells/cm^2. Six positive control and six negative control wells were additionally prepared, pipetting cells at the same density directly into cell culture-treated and non cell culture-treated 24-well plates respectively. Discs and controls were then incubated in complete culture medium for up to 48 hours.

The toxicity of membranes was investigated by comparing cell viability on the membranes with that on the positive control standard tissue-culture treated plates. In addition, cell affinity with each material was investigate by comparing the percentage of area covered by live cells on each membrane, with that on both positive and negative controls.

Both cell viability and cell coverage were determined at 24 h and 48 h (three discs of each material or control wells per time point). At the relevant time point, 2 μM/ml calcein AM and 10 μM/ml ethidium homodimer were added to each well for 30 min at 37 °C. Stained cells were observed under a fluorescence microscope, under 2.5x and 10x magnification at an excitation/emission of 488/526 nm (calcein AM) and 568/612 nm (ethidium homodimer) (Leica DM4000 B LED, Heidelberg, Germany). Matched images of samples were taken at the two wavelengths, in which calcein AM produced an intense uniform green fluorescence in live cells, while ethidium homodimer produced a bright red fluorescence in dead cells. At least three pictures were taken at random locations across the surface of each disc at each time point. The number of live cells (Lm) and dead cells (Dm) on the membrane disc, and live cells (Lw) and dead cells (Dw) in the well were counted in Image J (ImageJ software, NIH Image, MD, U.S.A.) and cell viability calculated using Eq. 1.

$$\textbf{Live cell ratio} = \frac{\boldsymbol{Lm+Lw}}{\boldsymbol{Lm+Lw+Dm+Dw}} \qquad \text{Eq. 1}$$

Cell coverage was also calculated using Image J (ImageJ software, NIH Image, MD, U.S.A.), dividing the area covered with cells by the whole area of the well. The cell viability and cell affinity analyses were repeated three times, with three different sets of membranes and controls, and tenocytes from three different bovine donors.

In vitro cell adhesion and morphology assay. Six sterilized discs of each membrane material (P1-P4), and six media-coated glass slides (positive controls) were placed, one disc per well, into two non cell culture-treated 24-well plates. Cell solution was pipetted directly onto the discs and slides, in order to seed them at a density of 4×10^4 cells/cm^2, and all samples incubated in complete culture medium for up to 48 hours. The cytoskeleton of cells on each electrospun membrane was compared with that of tenocytes cultured on media-coated glass slide surfaces (positive control) after 24 h and 48 h.

To visualise the cytoskeletal arrangement, cell coated discs and glass slides were washed twice in PBS, and then fixed in 4% paraformaldehyde for 10 minutes. After removing the fixative, cells were washed repeatedly in PBS, permeabilized with 0.1% Triton X-100 for 10 minutes, and then washed twice more in PBS. The actin cytoskeleton was then stained with Alexa Fluor 488 phalloidin (20 μg/mL) in PBS with 1% (wt) bovine serum albumin for 30 minutes, after which, cells were washed twice in PBS and the cell nucleus stained with DAPI (1 μg/mL) in PBS with 1%(wt) bovine serum albumin for 1 minute before a final wash in PBS. Samples were imaged under a confocal laser scanning microscope (Leica TCS SP2; Leica Microsystems, Heidelberg, Germany) at an excitation/emission of 488/526 nm (phalloidin) and 358/468 nm (DAPI). At least 3 matched pictures at each wavelength were taken for each sample at 40x magnification, and an additional picture digitally zoomed 3 times was taken, to show the morphology of a single cell.

The cytoskeletal analysis was repeated three times with three different sets of membranes and controls, and tenocytes from three different bovine donors.

Alamar blue assay. Three sterilized discs of each membrane were placed, one disc per well, into a cell culture-treated 24-well plate, and the 12 wells with membranes plus an additional three control wells were seeded with cells as previously described. Cell activity on each membrane and control well was investigated using an alamar blue assay after 24, 48 and 96 h. At the 24 hour time point, a 1/10 volume ratio of alamar blue reagent was added to the culture media of each well, and plates returned to the incubator for another 4 h. At this point, 100 μL of the alamar blue media mixture was taken from each sample well and its fluorescence was detected using a Fluo Star plate reader (BMG LABTECH®). At least 3 technical repeats were performed for each sample. After obtaining a reading, all media was discarded from each sample and control well, and fresh media was added, after which the plate was returned to the incubator. The same samples and control were subjected to repeat alamar blue assays at 48 h and 96 h following the same procedure, to monitor the cell activity over time. Activity of cells membranes was displayed normalized to the activity of the control samples. The alamar blue assay was repeated for three sets of membranes and controls, using tenocytes from three different bovine donors.

Statistical Analyses. Results are expressed either as mean ± SD or box whisker plots. The normality of the data was characterised using Shapiro-Wilk normality tests. For the live and dead assay, a one way ANOVA was performed followed by Tukey comparison of means, while for viable cell coverage and alamar blue analysis, due to the non-normal distribution of the data, Kruskal-Wallis tests were performed followed by Dunn's tests using statistical analysis software Graphpad Prism 6.0 (GraphPad Software, San Diego, CA). Unless otherwise stated, $p < 0.05$ was considered significant.

Supporting Information

^{1}H NMR of the polymers, the comparison between fibre diameters and water contact angles of different membranes, and the comparison of cell activity between different membranes and at different time points are provided in the supporting information.

Author information

Corresponding Authors

*Email: r.becer@qmul.ac.uk.

*Email: h.r.c.screen@qmul.ac.uk.

ORCID ID: https://orcid.org/0000-0003-0968-6662

Acknowledgements

The first author gratefully acknowledges the financial support from the China Scholarship Council (CSC) and Queen Mary, University of London and technical support from all the group members in Dr Becer research group and Prof Screen research group.

Conflicts of interest

The authors declare no conflict of interest.

ABBREVIATIONS

PCL, poly (ε-caprolactone); PLA, poly(lactic acid); PGA, poly(glycolic acid); FDA, Food and Drug Administration; ROP, ring opening polymerization; ATRP, atom transfer radical polymerization; Sn(Oct)2, Tin(II) 2-ethylhexanoate; TEA, trimethylamine; Al2O3, aluminium oxide; PMDETA, N,N,N',N'',N''-Pentamethyldiethylenetriamine; DAPI, 4',6-Diamidino-2-Phenylindole, Dihydrochloride; ε-CL, ε-caprolactone; PFS, 2,3,4,5,6-pentafluorostyrene; NMR, Nuclear Magnetic Resonance; CDCl3, chloroform; DMSO-d6,

deuterated dimethyl sulfoxide; GPC, Gel Permeation Chromatography; DMF, dimethylformamide; THF, Tetrahydrofuran; PTFE, Polytetrafluoroethylene; SEM, scanning electron microscopy; SD, standard deviation; WCA, water contact angle; DMEM, Dulbecco's Modified Eagle Medium; HEPES, N-2-hydroxyethylpiperazine-N-2-ethane sulfonic acid.

References

(1) Hollister, S. J. (2005) Porous scaffold design for tissue engineering. *Nat. Mater. 4*, 518-524.

(2) Causa, F., Netti, P. A., and Ambrosio, L. (2007) A multi-functional scaffold for tissue regeneration: the need to engineer a tissue analogue. *Biomaterials 28*, 5093-5099.

(3) Screen, H. R., Chhaya, V. H., Greenwald, S. E., Bader, D. L., Lee, D. A., and Shelton, J. C. (2006) The influence of swelling and matrix degradation on the microstructural integrity of tendon. *Acta. Biomater. 2*, 505-513.

(4) Tchemtchoua, V. T., Atanasova, G., Aqil, A., Filée, P., Garbacki, N., Vanhooteghem, O., Deroanne, C., Noël, A., Jérome, C., and Nusgens, B. (2011) Development of a chitosan nanofibrillar scaffold for skin repair and regeneration. *Biomacromolecules 12*, 3194-3204.

(5) Weiner, S., and Wagner, H. D. (1998) The material bone: structure-mechanical function relations. *Annual Review of Materials Science 28*, 271-298.

(6) Anselme, K., Davidson, P., Popa, A., Giazzon, M., Liley, M., and Ploux, L. (2010) The interaction of cells and bacteria with surfaces structured at the nanometre scale. *Acta. Biomater. 6*, 3824-3846.

(7) Bettinger, C. J., Langer, R., and Borenstein, J. T. (2009) Engineering substrate topography at the micro-and nanoscale to control cell function. *Angew. Chem. Int. Ed. 48*, 5406-5415.

(8) Al-Namnam, N. M. N., Kim, K. H., Chai, W. L., Ha, K. O., Siar, C. H., and Ngeow, W. C. (2016) Modified poly (caprolactone trifumarate) with embedded gelatin microparticles as a functional scaffold for bone tissue engineering. *J. Appl. Polym. Sci. 133*.

(9) Liu, S., Zhao, J., Ruan, H., Tang, T., Liu, G., Yu, D., Cui, W., and Fan, C. (2012) Biomimetic sheath membrane via electrospinning for antiadhesion of repaired tendon. *Biomacromolecules 13*, 3611-3619.

(10) Fallahiarezoudar, E., Ahmadipourroudposht, M., Idris, A., Yusof, N. M., Marvibaigi, M., and Irfan, M. (2016) Characterization of maghemite (γ-Fe2O3)-loaded poly-l-lactic acid/thermoplastic polyurethane electrospun mats for soft tissue engineering. *J. Mater. Sci. 51*, 1-21.

(11) Kim, M., Hong, B., Lee, J., Kim, S. E., Kang, S. S., Kim, Y. H., and Tae, G. (2012) Composite system of PLCL scaffold and heparin-based hydrogel for regeneration of partial-thickness cartilage defects. *Biomacromolecules 13*, 2287-2298.

(12) Xu, C., Inai, R., Kotaki, M., and Ramakrishna, S. (2004) Aligned biodegradable nanofibrous structure: a potential scaffold for blood vessel engineering. *Biomaterials 25*, 877-886.

(13) Li, W. J., Laurencin, C. T., Caterson, E. J., Tuan, R. S., and Ko, F. K. (2002) Electrospun nanofibrous structure: a novel scaffold for tissue engineering. *J. Biomed. Mater. Res. Part B Appl. Biomater 60*, 613-621.

(14) Rogina, A., Pribolšan, L., Hanžek, A., Gómez-Estrada, L., Ferrer, G. G., Marijanović, I., Ivanković, M., and Ivanković, H. (2016) Macroporous poly (lactic acid) construct supporting the osteoinductive porous chitosan-based hydrogel for bone tissue engineering. *Polymer 98*, 172-181.

(15) Kim, S. H., Misner, M. J., Xu, T., Kimura, M., and Russell, T. P. (2004) Highly oriented and ordered arrays from block copolymers via solvent evaporation. *Adv. Mater. 16*, 226-231.

(16) Bhardwaj, N., and Kundu, S. C. (2010) Electrospinning: a fascinating fiber fabrication technique. *Biotechnol. Adv. 28*, 325-347.

(17) Hutmacher, D. W. (2000) Scaffolds in tissue engineering bone and cartilage. *Biomaterials 21*, 2529-2543.

(18) Lutolf, M., and Hubbell, J. (2005) Synthetic biomaterials as instructive extracellular microenvironments for morphogenesis in tissue engineering. *Nat. Biotechnol. 23*, 47-55.

(19) Lee, K. Y., and Mooney, D. J. (2001) Hydrogels for tissue engineering. *Chem. Rev. 101*, 1869-1880.

(20) Yang, F., Murugan, R., Wang, S., and Ramakrishna, S. (2005) Electrospinning of nano/micro scale poly (L-lactic acid) aligned fibers and their potential in neural tissue engineering. *Biomaterials 26*, 2603-2610.

(21) Park, K. E., Kang, H. K., Lee, S. J., Min, B.-M., and Park, W. H. (2006) Biomimetic nanofibrous scaffolds: preparation and characterization of PGA/chitin blend nanofibers. *Biomacromolecules 7*, 635-643.

(22) Williams, J. M., Adewunmi, A., Schek, R. M., Flanagan, C. L., Krebsbach, P. H., Feinberg, S. E., Hollister, S. J., and Das, S. (2005) Bone tissue engineering using polycaprolactone scaffolds fabricated via selective laser sintering. *Biomaterials 26*, 4817.

(23) Luu, Y., Kim, K., Hsiao, B., Chu, B., and Hadjiargyrou, M. (2003) Development of a nanostructured DNA delivery scaffold via electrospinning of PLGA and PLA–PEG block copolymers. *J. Control. Release 89*, 341-353.

(24) Guarino, V., Causa, F., Taddei, P., di Foggia, M., Ciapetti, G., Martini, D., Fagnano, C., Baldini, N., and Ambrosio, L. (2008) Polylactic acid fibre-reinforced polycaprolactone scaffolds for bone tissue engineering. *Biomaterials 29*, 3662-3670.

(25) Lendlein, A., and Langer, R. (2002) Biodegradable, elastic shape-memory polymers for potential biomedical applications. *Science 296*, 1673-1676.

(26) Böstman, O., and Pihlajamäki, H. (2000) Clinical biocompatibility of biodegradable orthopaedic implants for internal fixation: a review. *Biomaterials 21*, 2615-2621.

(27) Temenoff, J. S., and Mikos, A. G. (2000) Review: tissue engineering for regeneration of articular cartilage. *Biomaterials 21*, 431-440.

(28) Lam, C. X., Hutmacher, D. W., Schantz, J. T., Woodruff, M. A., and Teoh, S. H. (2009) Evaluation of polycaprolactone scaffold degradation for 6 months in vitro and in vivo. *J. Biomed. Mater. Res. A 90*, 906-919.

(29) Zhang, H., Lin, C.-Y., and Hollister, S. J. (2009) The interaction between bone marrow stromal cells and RGD-modified three-dimensional porous polycaprolactone scaffolds. *Biomaterials 30*, 4063-4069.

(30) Wang, Y.-C., Kao, S.-H., and Hsieh, H.-J. (2003) A chemical surface modification of chitosan by glycoconjugates to enhance the cell-biomaterial interaction. *Biomacromolecules 4*, 224-231.

(31) Zhang, Y., Venugopal, J., Huang, Z.-M., Lim, C., and Ramakrishna, S. (2005) Characterization of the surface biocompatibility of the electrospun PCL-collagen nanofibers using fibroblasts. *Biomacromolecules 6*, 2583-2589.

(32) Angarano, M., Schulz, S., Fabritius, M., Vogt, R., Steinberg, T., Tomakidi, P., Friedrich, C., and Mülhaupt, R. (2013) Layered gradient nonwovens of in situ crosslinked electrospun collagenous nanofibers used as modular scaffold systems for soft tissue regeneration. *Adv. Funct. Mater. 23*, 3277-3285.

(33) Lancuški, A., Bossard, F. d. r., and Fort, S. b. (2013) Carbohydrate-decorated PCL fibers for specific protein adhesion. *Biomacromolecules 14*, 1877-1884.

(34) Chen, C.-H., Chen, S.-H., Shalumon, K., and Chen, J.-P. (2015) Dual functional core–sheath electrospun hyaluronic acid/polycaprolactone nanofibrous membranes embedded with silver nanoparticles for prevention of peritendinous adhesion. *Acta. Biomater. 26*, 225-235.

(35) Russo, L., Russo, T., Battocchio, C., Taraballi, F., Gloria, A., D'Amora, U., De Santis, R., Polzonetti, G., Nicotra, F., and Ambrosio, L. (2015) Galactose grafting on poly (ε-caprolactone) substrates for tissue engineering: a preliminary study. *Carbohydr. Res. 405*, 39-46.

(36) Lu, J., Zhang, W., Richards, S.-J., Gibson, M. I., and Chen, G. (2014) Glycopolymer-coated gold nanorods synthesised by a one pot copper (0) catalyzed tandem RAFT/click reaction. *Polym. Chem. 5*, 2326-2332.

(37) Lou, S.-F., Wang, L., Williams, G. R., Nie, H., Quan, J., and Zhu, L. (2014) Galactose functionalized injectable thermoresponsive microgels for sustained protein release. *Colloids Surf., B 113*, 368-374.

(38) Kurtulus, I., Yilmaz, G., Ucuncu, M., Emrullahoglu, M., Becer, C. R., and Bulmus, V. (2014) A new proton sponge polymer synthesized by RAFT polymerization for intracellular delivery of biotherapeutics. *Polym. Chem. 5*, 1593-1604.

(39) Wang, L., Williams, G. R., Nie, H.-l., Quan, J., and Zhu, L.-m. (2014) Electrospun glycopolymer fibers for lectin recognition. *Polym. Chem. 5*, 3009-3017.

(40) Liu, J., Duong, H., Whittaker, M. R., Davis, T. P., and Boyer, C. (2012) Synthesis of functional core, star polymers via RAFT polymerization for drug delivery applications. *Macromol. Rapid Commun. 33*, 760-766.

(41) Wei, X., Luo, Q., Sun, L., Li, X., Zhu, H., Guan, P., Wu, M., Luo, K., and Gong, Q. (2016) Enzyme-and pH-Sensitive Branched Polymer–Doxorubicin Conjugate-Based

Nanoscale Drug Delivery System for Cancer Therapy. *ACS Appl. Mater. Interfaces 8*, 11765-11778.

(42) Zhou, X., Zheng, Q., Wang, C., Xu, J., Wu, J., Kirk, T. B., Ma, D., and Xue, W. (2016) Star-shaped amphiphilic hyperbranched polyglycerol-conjugated with dendritic poly (L-lysine) for the co-delivery of docetaxel and MMP-9 siRNA in cancer therapy. *ACS Appl. Mater. Interfaces*.

(43) Teo, J., McCarroll, J. A., Boyer, C., Youkhana, J., Sagnella, S. M., Duong, H. T., Liu, J., Sharbeen, G., Goldstein, D., and Davis, T. P. (2016) A rationally optimized nanoparticle system for the delivery of RNA interference therapeutics into pancreatic tumors in vivo. *Biomacromolecules 17*, 2337-2351.

(44) Isono, T., Miyachi, K., Satoh, Y., Nakamura, R., Zhang, Y., Otsuka, I., Tajima, K., Kakuchi, T., Borsali, R., and Satoh, T. (2016) Self-Assembly of Maltoheptaose-block-polycaprolactone Copolymers: Carbohydrate-Decorated Nanoparticles with Tunable Morphology and Size in Aqueous Media. *Macromolecules 49*, 4178-4194.

(45) Fukukawa, K.-i., Rossin, R., Hagooly, A., Pressly, E. D., Hunt, J. N., Messmore, B. W., and Hawker, C. J. (2008) Synthesis and characterization of core–shell star copolymers for in vivo PET imaging applications. *Biomacromolecules 9*, 1329-1339.

(46) Bagby, T. R., Duan, S., Cai, S., Yang, Q., Thati, S., Berkland, C., Aires, D. J., and Forrest, M. L. (2012) Lymphatic trafficking kinetics and near-infrared imaging using star polymer architectures with controlled anionic character. *Eur. J. Pharm. Sci. 47*, 287-294.

(47) Yilmaz, G., and Becer, C. R. (2015) Glyconanoparticles and their interactions with lectins. *Polym. Chem. 6*, 5503-5514.

(48) El-Boubbou, K., Zhu, D. C., Vasileiou, C., Borhan, B., Prosperi, D., Li, W., and Huang, X. (2010) Magnetic glyco-nanoparticles: a tool to detect, differentiate, and unlock the glyco-codes of cancer via magnetic resonance imaging. *J. Am. Chem. Soc. 132*, 4490-4499.

(49) Zhang, Q., Collins, J., Anastasaki, A., Wallis, R., Mitchell, D. A., Becer, C. R., and Haddleton, D. M. (2013) Sequence-Controlled Multi-Block Glycopolymers to Inhibit DC-SIGN-gp120 Binding. *Angew. Chem. Int. Ed. 52*, 4435-4439.

(50) Smith, R., McIlwraith, W., Schweitzer, R., Kadler, K., Cook, J., Caterson, B., Dakin, S., Heinegård, D., Screen, H., and Stover, S. (2014) Advances in the understanding of tendinopathies: A report on the second havemeyer workshop on equine tendon disease. *Equine. Vet. J 46*, 4-9.

(51) Peffers, M. J., Thorpe, C. T., Collins, J. A., Eong, R., Wei, T. K., Screen, H. R., and Clegg, P. D. (2014) Proteomic analysis reveals age-related changes in tendon matrix composition, with age-and injury-specific matrix fragmentation. *J. Biol. Chem. 289*, 25867-25878.

(52) Hosono, N., Gochomori, M., Matsuda, R., Sato, H., and Kitagawa, S. (2016) Metal–Organic Polyhedral Core as a Versatile Scaffold for Divergent and Convergent Star Polymer Synthesis. *J. Am. Chem. Soc. 138*, 6525-6531.

(53) Aksakal, R., Resmini, M., and Becer, C. (2016) Pentablock star shaped polymers in less than 90 minutes via aqueous SET-LRP. *Polym. Chem. 7*, 171-175.

(54) Becer, C. R., Babiuch, K., Pilz, D., Hornig, S., Heinze, T., Gottschaldt, M., and Schubert, U. S. (2009) Clicking pentafluorostyrene copolymers: synthesis, nanoprecipitation, and glycosylation. *Macromolecules 42*, 2387-2394.

(55) Babiuch, K., Becer, C. R., Gottschaldt, M., Delaney, J. T., Weisser, J., Beer, B., Wyrwa, R., Schnabelrauch, M., and Schubert, U. S. (2011) Adhesion of Preosteoblasts and Fibroblasts onto Poly (pentafluorostyrene)-Based Glycopolymeric Films and their Biocompatibility. *Macromol. Biosci. 11*, 535.

(56) Li, M., Mondrinos, M. J., Gandhi, M. R., Ko, F. K., Weiss, A. S., and Lelkes, P. I. (2005) Electrospun protein fibers as matrices for tissue engineering. *Biomaterials 26*, 5999-6008.

(57) Zhang, X., MacDonald, D. A., Goosen, M. F., and McAuley, K. B. (1994) Mechanism of lactide polymerization in the presence of stannous octoate: the effect of hydroxy and carboxylic acid substances. *J. Polym. Sci. A Polym. Chem. 32*, 2965-2970.

(58) Patel, D., Sharma, S., Bryant, S. J., and Screen, H. R. (2016) Recapitulating the Micromechanical Behavior of Tension and Shear in a Biomimetic Hydrogel for Controlling Tenocyte Response. *Adv. Healthc. Mater.*

Table of contents graphic